European Journal of Medicinal Chemistry 62 (2013) 139–147

Contents lists available at SciVerse ScienceDirect

European Journal of Medicinal Chemistry

journal homepage: http://www.elsevier.com/locate/ejmech

Original article

Synthesis, characterization, cytotoxicity and antimicrobial studies on bis(*N*-furfuryl-*N*-(2-phenylethyl)dithiocarbamato-*S*,*S*′)zinc(II) and its nitrogen donor adducts

Palanisamy Jamuna Rani, Subbiah Thirumaran*

Department of Chemistry, Annamalai University, Annamalainagar 608 002, Tamil Nadu, India

ARTICLE INFO

Article history:
Received 28 July 2012
Received in revised form
2 December 2012
Accepted 31 December 2012
Available online 7 January 2013

Keywords:
Dithiocarbamate
Nitrogen donor ligands
Zinc(II)
X-ray structure
HeLa cell line
Antimicrobial studies

ABSTRACT

[Zn(fpedtc)$_2$] (**1**), [Zn(fpedtc)$_2$(py)] (**2**), [Zn(fpedtc)$_2$(1,10-phen)] (**3**) and [Zn(fpedtc)$_2$(2,2′-bipy)] (**4**) (where fpedtc = *N*-furfuryl-*N*-(2-phenylethyl)dithiocarbamate, py = pyridine, 1,10-phen = 1,10-phenanthroline and 2,2′-bipy = 2,2′-bipyridine) were synthesized. Characterization of the complexes were achieved by IR and NMR (^{1}H and ^{13}C) spectra and in addition, for **2** and **3**, by X-ray crystallography. Single crystal X-ray structural analysis of **2** and **3** showed that complex **2** is almost half way between trigonal bipyramidal and square pyramidal and complex **3** has a distorted octahedral geometry. Zn–N distances in **2** is shorter than that found in a six coordinate complex **3** due to the change in coordination number. These complexes were also screened for *in vitro* antibacterial and antifungal activities and significant activities have been found. *In vitro* cytotoxic activity of all the synthesized complexes was evaluated on HeLa cell line. Complex **1** exhibits maximum inhibitory effect at a concentration of 40 μg mL^{-1} on HeLa cell line.

1. Introduction

Dithiocarbamates have a wide range of applications in medicine, industry and rubber vulcanization [1–4], and can serve as antioxidants for increasing the longevity and photo-stability of a variety of polymers, oils and other materials [5]. Metal dithiocarbamate complexes and their nitrogen donor adducts are useful precursors for the synthesis metal sulfide nanoparticles [6,7].

Several dithiocarbamate salts and metal complexes of dithiocarbamates have been used as agrochemicals, mainly due to their high efficiency in controlling plant fungal diseases and their relatively low toxicity [8–13]. Cervical carcinoma significantly affects women world wide, especially in developing countries [14]. Approximately, 500,000 cases of cervical cancer diagnosed per year with nearly 40% of those resulting in death [15]. Although cancer has existed as a disease since prehistoric time, it is still one of the major causes of death in the world. To date, the most reliable way to reduce or cure cancer is to remove and/or to block the fast proliferating malignant tissues. The discovery of cisplatin (cis-[Pt(NH$_3$)$_2$Cl$_2$]), the first inorganic compound to block DNA replication and cell division, has demonstrated that metal complexes can play an important role in the treatment of cancer opening up new perspectives in anticancer research based on metallopharmaceuticals [16]. Despite high nephrotoxicity, neurotoxicity and acquired drug resistance as major drawbacks, cisplatin and its two analogs (carboplatin and oxaliplatin), are among the most effective chemotherapeutic agents in clinical use to date [17]. Dithiocarbamates have been evaluated for their efficiency as inhibitors of cisplatin-induced nephrotoxicity [18]. In particular, dithiocarbamates selectively protects normal tissue without inhibiting the antitumor effect [19,20]. The majority of the dithiocarbamate [M(S$_2$CNR^{1}R^2)$_n$] complexes studied have simple R^1 and R^2 groups such as methyl, ethyl and phenyl [21]. Only one structural report has been made on furfuryl based dithiocarbamate complex from our laboratory [22].

To understand the influence of furfuryl based dithiocarbamate and nitrogen donor ligands (py, 1,10-phen, 2,2-bipy) on biological properties, we report results on cytotoxicity, antifungal and antibacterial properties of complexes **1**–**4**, as well as their IR and NMR spectra. In addition, the crystal structures of **2** and **3** are described.

2. Results and discussion

2.1. Synthesis of complexes 1–4 and their characterization

Complexes **1**–**4** were prepared according to the synthetic procedure shown in Schemes 1 and 2. Furfuraldehyde was condensed

* Corresponding author. Tel.: +91 9842897597.
E-mail address: sthirumaran@yahoo.com (S. Thirumaran).

0223-5234/$ – see front matter © 2013 Elsevier Masson SAS. All rights reserved.
http://dx.doi.org/10.1016/j.ejmech.2012.12.047

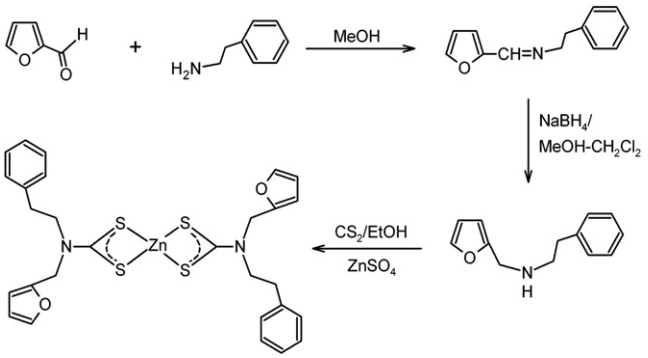

Scheme 1. Preparation of complex **1**.

with 2-phenylethylamine to form the imine. Sodium borohydride reduction of imine in methanol–dichloromethane afforded *N*-furfuryl-*N*-(2-phenylethyl)amine as yellow oil. Complex **1** was prepared from amine in EtOH by reaction with carbon disulfide and $ZnSO_4$ in water. The reaction of complex **1** with nitrogen donor ligands (py, 1,10-phen, 2,2′-bipy) yielded **2**, **3** and **4**. The complexes are quite stable at ambient conditions. They are soluble in chloroform, dichloromethane and acetonitrile and insoluble in ethanol, methanol and water.

IR spectroscopy has been used to understand the nature of coordination mode (monodentate or bidentate) of dithiocarbamate moiety. IR spectra of complexes **1** and **2** are given in Fig. 1. Based on Bonati et al. criterion, the presence of only one characteristic band in the region 1050–900 cm^{-1}, the ν_{C-S} mode, is due to bidentate coordination of the dithiocarbamate group while a split band within narrow range of 20 cm^{-1} is indicative of the monodentate nature of the dithiocarbamate group [23]. In the present study, the C–S stretching vibrations are observed in the region 1017–1014 cm^{-1} without any splitting, supporting the bidentate coordination of the dithiocarbamate ligand. The dithiocarbamate compounds exhibit another characteristic band in the region 1550–1450 cm^{-1} assignable to the ν_{C-N} (thioureide) [24]. The infrared spectra of **1**–**4** show ν_{C-N} (thioureide) bands in the region 1487–1462 cm^{-1}, indicating the partial double bond character.

The thioureide ν_{C-N} bands of complexes follow the order **1** > **2** > **3** ≈ **4**. This indicates that the $N^{\delta+}\cdots C^{\delta-}$ double bond character decreases with increasing coordination number [25]. The characteristic band due to pyridine appears at 1604 cm^{-1} in **2**. The ring frequencies associated with 1,10-phenanthroline and 2,2′-bipyridine are 1600–1000 cm^{-1} [26]. In this study 1,10-phenanthroline adduct **3** shows bands at 1584 and 1507 cm^{-1} whereas 2,2′-bipyridine adduct **4** reveals bands at 1600 and 1567 cm^{-1}. Other bands due to nitrogen ligands are masked by those due to dithiocarbamate.

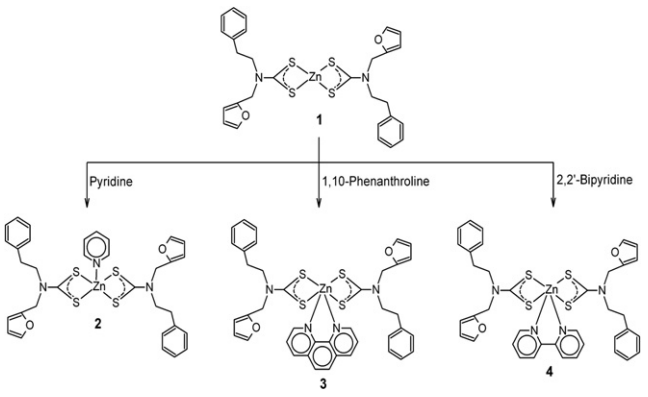

Scheme 2. Preparation of complexes **2**, **3** and **4**.

^1H NMR spectrum of *N*-furfuryl-*N*-(2-phenylethyl)amine shows a singlet at 3.68 ppm and two triplets at 2.72 and 2.79 ppm due to methylene protons of furfuryl group and the ethylene unit of 2-phenylethyl group, respectively; that shifted to lower field being nitrogen bound. The signal of methylene protons (singlet) of N–CH_2 (furfuryl) appears in the region 4.95–5.12 ppm in all the complexes **1**–**4**. All the complexes showed two equal intensity triplets in the aliphatic region 3.00–4.10 ppm associated with the ethylene unit of 2-phenylethyl group; that shifted to lower field being nitrogen bound. The nitrogen bound methylene proton signals of complexes **1**–**4** are strongly deshielded compared to those of free *N*-furfuryl-*N*-(2-phenylethyl)amine, which confirms the formation of dithiocarbamate.

Complexes **1**–**4** show $N^{13}CS_2$ signals in the region 205.2–207.1 ppm, indicating contribution of double bond character to a formally single N–C bond in the dithiocarbamate. The $N^{13}CS_2$ chemical shift of dithiocarbamate is also affected by coordination of nitrogen donor to metal. Additional coordination of nitrogen donors to metal dithiocarbamates yields a decrease of nitrogen–carbon partial double bond character and, as a result of that, the $N^{13}CS_2$ carbon of nitrogen donor adducts **2**–**4** are additionally deshielded compared to parent complex **1**.

2.2. Structural studies on complexes *2* and *3*

An ORTEP diagram of complex **2** is shown in Fig. 2. Complex **2** contains four discrete molecules per unit cell. The zinc atom in complex **2** is five coordinated to four sulfur atoms from the dithiocarbamates and to one nitrogen atom from pyridine. The coordination group around zinc is distorted trigonal bipyramid with coplanar atoms Zn, N(pyridine), S(1) and S(1^i) lying in the equatorial plane and S(2) and S(2^i) occupying the axial positions. In this complex, dithiocarbamate ligands are bound in a chelating fashion that bridge equatorial and axial sites. The two dithiocarbamate ligands in **2** coordinate in an anisobidentate fashion [Zn–S1 = 2.3600(7) and Zn–S2 = 2.5621(6) Å]. The C–S distances are slightly asymmetric and the shorter Zn–S1 bond is associated with longer C–S distance. The structure of complex **2** is intermediate between the tetragonal pyramid (TP) and trigonal bipyramidal. For accurate description of the geometry, this complex is characterized by using the τ descriptor for five coordination suggested by Addison et al. [27]. From the τ values, the coordination geometry is described as being 56% along the pathway of distortion from square pyramid toward trigonal bipyramid. The short thioureide C–N distance [1.339(3) Å], indicates that the π-electron density is delocalized over the S_2CN moiety and this bond has a significant double bond character. All the C–S bonds in the present structure are of partial double bond character as observed in other dithiocarbamate complexes [28].

The ORTEP diagram of complex **3** is shown in Fig. 3. Zinc is hexacoordinated by two nitrogen atoms from 1,10-phenanthroline and four sulfur from the chelating dithiocarbamate groups. In this complex, the zinc atom is situated at the center of a distorted tetragonal bipyramidal arrangement with two sulfur atoms from dithiocarbamate groups [S1, S3] and two nitrogen atoms from the 1,10-phenanthroline ligand [N3, N4] on the basal plane and the two remaining sulfur atoms as vertices. The two bonds Zn–S2 and Zn–S4 are relatively longer than others due to the steric influence of the 1,10-phenanthroline ligand. The two S–Zn–S angles [S2–Zn–S4 = 170.54(2) and S1–Zn–S3 = 101.93(2)°] correspond to *trans* and *cis* octahedral values, respectively. The N4–Zn–N3 angle observed in the adduct is 75.18(7)°. The short thioureide C–N distance [1.373(3) Å] indicates that the π-electron density is delocalized over the S_2CN

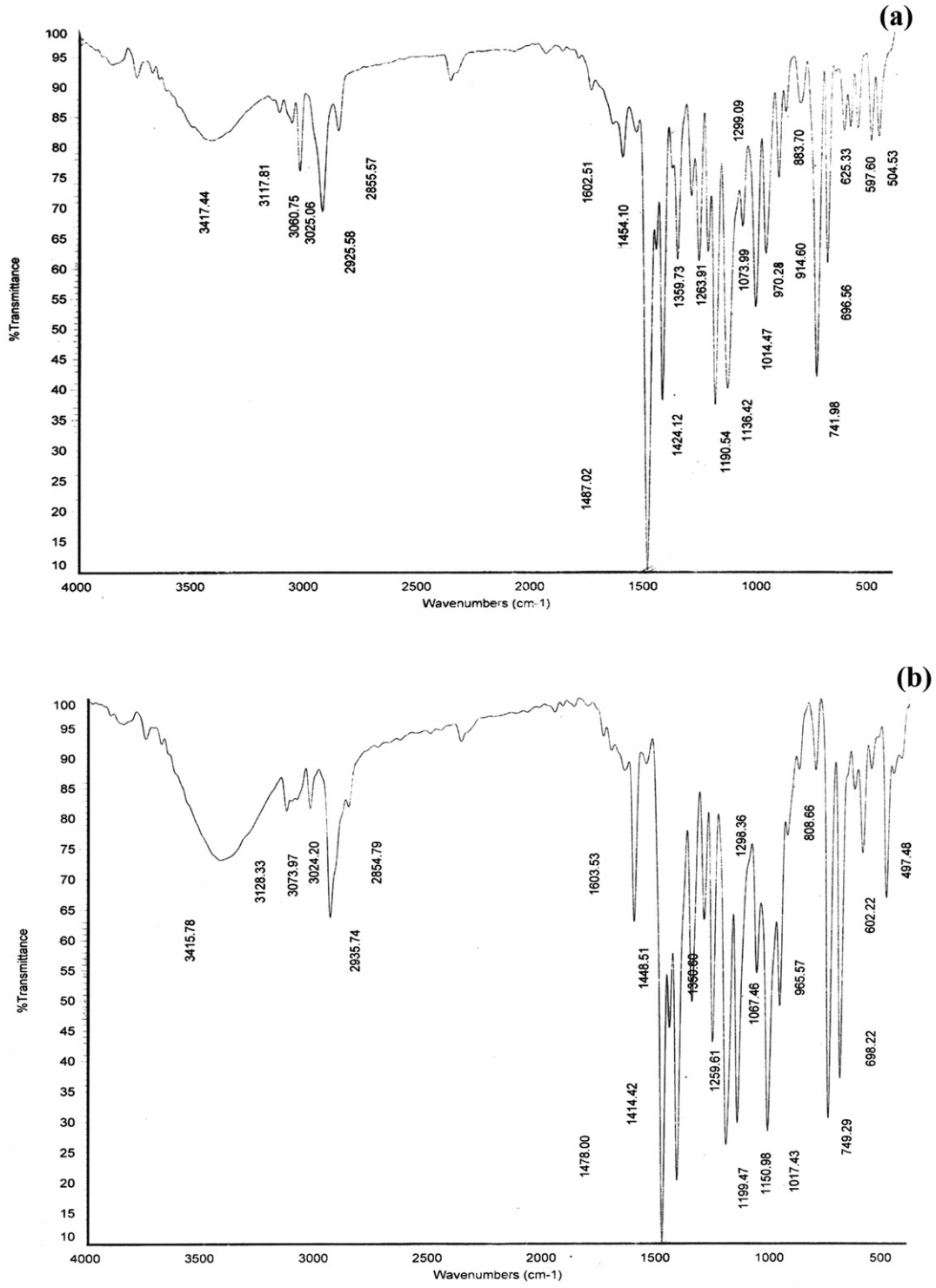

Fig. 1. IR spectra of complexes **1** and **2**.

moiety and this bond has double bond character comparing well with the adjacent typical single bonded N–C distance [C(16)–N(3) = 1.473(3) Å]. The S–Zn–S bite angles in **3** are less compared to those observed in **2** due to the increased coordination around zinc. Reduction in S–Zn–S bite angles has resulted in a change in Zn–S distances. No significant changes in C–S, N–C bond distances and S–C–S angles are observed. The Zn–N distance in **3** is longer than that found in **2** due to the increased coordination number.

2.3. Biological activity

2.3.1. Antibacterial activity

The disc diffusion assay was conducted to determine if the tested compounds could inhibit the growth of bacteria. The antibacterial activity of the complexes has been screened against *Escherichia coli*, *Salmonella typhi*, *Vibrio cholerae* and *Staphylococcus aureus*. The results are given in Table 1. Significant antibacterial

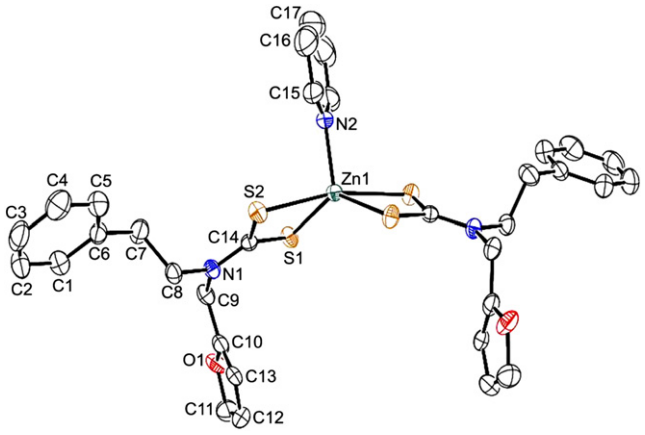

Fig. 2. ORTEP diagram of **2** (hydrogen atoms have been omitted for clarity).

activities were observed when compared to a standard drug Chloramphenicol. Complex **3** exhibits less activity against all the tested bacteria. Complex **4** is more toxic for all the tested *Gram negative* bacteria compared to other complexes **1**–**3**. Data obtained also indicate the increasing dosage level of complexes from 100 to 400 μg/disc, the inhibitory effect slightly increased.

The minimum inhibitory concentrations are given in Table 2. Complex **4** was found to be the most effective against the tested *Gram negative* pathogenic strains of bacteria *E. coli*, *S. typhi* and *V. cholera* with MIC values of 25, 25 and 3.12 μg/mL, respectively and less active against the tested *Gram positive* pathogenic strain of *S. aureus*. The antibacterial activity of **4** is more active than the other complexes, suggesting 2,2′-bipyridine assist the action of complex against *Gram negative* bacteria possibly via enhanced membrane transport into the cell or some other mode of action [29]. Complex **2** exhibited greater inhibitory action against *S. aureus* (25 μg/mL) than other complexes.

2.3.2. Antifungal activity

The antifungal activities of the complexes using *Microsporum gypseum*, *Trichophyton rubrum*, *Epidermophyton floccosum* and *Trichophyton mentagrophyte* were studied *in vitro* and results are summarized in Table 3. The antifungal activity of the compounds as compared with that of reference drug (Chloramphenicol) showed significant activity. Complex **1** was found to exhibit maximum

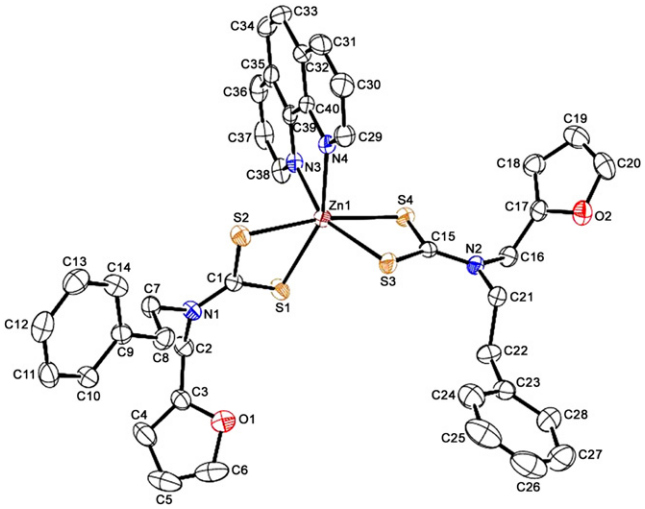

Fig. 3. ORTEP diagram of **3** (hydrogen atoms have been omitted for clarity).

Table 1
Antibacterial activity (diameter of inhibition zone (cm)) of complexes **1**–**4** against four different bacterial pathogens.

Selected bacteria	Chloramphenicol (100 μg)	Complex				Disc content (μg/disc)
		1	**2**	**3**	**4**	
Escherichia coli	1.9	0.9	1.0	0.5	0.9	100
		1.0	1.5	1.0	1.5	400
Salmonella typhi	2.0	0.8	0.8	0.7	0.9	100
		1.2	1.3	1.1	1.5	400
Vibrio cholerae	2.0	0.8	1.2	0.5	1.7	100
		1.4	1.4	0.8	1.9	400
Staphylococcus aureus	2.2	0.6	0.9	–	0.6	100
		1.0	1.5	0.8	1.5	400

activity against *M. gypseum* and *T. rubrum* when compared with other complexes. Complexes **2** and **4** also showed good activity against *T. rubrum*. All the complexes revealed very less activity against *E. floccosum*. Complex **4** exhibited more activity against *T. mentagrophyte*.

Complex **1** against *M. gypseum* and *T. rubrum* explored good inhibitory activity (3.12 and 25 μg/mL, respectively). All the complexes did not show any inhibitory activity against *E. floccosum* even at concentration of 50 μg/mL. Complexes **3** and **4** revealed good inhibitory effect against *T. mentagrophyte* with MIC value of 6.25 μg/mL. The antifungal activity of dithiocarbamates may be attributed to their ability to chelate with metal ions. When these metal complexes penetrates lipid barriers in the fungal cell and may be ultimate toxicant or alternatively, it may be converted into free dithiocarbamate anions, which complexing with trace metals and thus depriving the cell of the needed metal ion and therefore causes death of fungal cell.

2.3.3. Cytotoxicity results

All the synthesized complexes **1**–**4** were examined for their cytotoxic properties on HeLa cell line by means of MTT test that allows us to evaluate the toxic effect of complexes on cellular mitochondrial metabolism. Cells were tested for 48 h with increasing concentrations of tested compounds. Cytotoxicity results are given in Table 4. Microscopic images of control cancer cells and apoptotic morphological changes in HeLa cell line treated with complex **1**–**4** are shown in Fig. 4. The results clearly show concentration dependent inhibition of cancer cell by all the complexes. Complex **1** exhibits a satisfactory inhibitory effect on cell proliferation. A maximum inhibitory effect of complex **1** is observed at a concentration of 40 μg mL^{-1}. Complexes **2**–**4** showed lower cytotoxic effect than complex **1**. This is because the complex **1** exists as four coordinated with distorted tetrahedral geometry which will enhance the cytotoxic activity of complex **1**. This is in consistent with literature that species having the tetrahedral geometry are more active [30].

3. Conclusion

New complexes **1**–**4** have been synthesized, and characterized by elemental analysis and spectroscopic studies. Single crystal X-ray structural analysis were carried out for **2** and **3**. The Zn–N distance in **3** is longer than that found in **2** due to the increased coordination around zinc. The antimicrobial activities of all complexes were analyzed at the concentrations 100 and 400 μg mL^{-1}. All the complexes exhibit antibacterial activity against four bacterial species. Complex **4** has greater activity than other tested complexes and has almost equal activity against *E. coli*, *S. typhi*, *V. cholerae* and *S. aureus* as compared with the Chloramphenicol. These complexes were also screened for *in vitro* antifungal activity. Complex 1 against *M. gypseum* and *T. rubrum* and complexes **1** and

Table 2
Antimicrobial activity (minimum inhibitory concentration (MIC) in μg/mL) of complexes **1**–**4**.

Complex	Minimum inhibitory concentration (MIC) in μg/mL							
	Bacterial strains				Fungal strains			
	E. coli	*S. typhi*	*V. cholerae*	*S. aureus*	*M. gypseum*	*T. rubrum*	*E. floccosum*	*T. mentagrophyte*
1	25	50	50	100	3.12	25	200	50
2	25	50	12.5	25	25	100	100	12.5
3	100	50	100	>200	>200	50	>200	6.25
4	25	25	3.12	100	25	50	200	6.25
Chloramphenicol	12.5	6.25	6.25	3.12	25	12.5	6.25	3.12

4 against *T. mentagrophyte* have been found to exhibit maximum inhibitory effect. Complex **1** has potent *in vitro* cytotoxic against HeLa cell line.

4. Experimental

All reagents and solvents were commercially available high-grade materials (Merck/sd Fine/Himedia) and used as received. IR spectra were recorded on a Thermo Nicolet Avatar 330 FT-IR spectrophotometer (range 400–4000 cm^{-1}) as KBr pellets. The NMR spectra were recorded on Bruker 400/100 and 500/125 MHz NMR spectrometers at room temperature in $CDCl_3$, using TMS as internal reference.

4.1. X-ray crystallography

Diffraction data for **2** and **3** were recorded on an Bruker axs kappa apex2CCD diffractometer using graphite monochromated MoK_α radiation (λ = 0.71073 Å) at ambient temperature. The structure was solved by SIR-92 [31] and refined by full matrix least square with SHELXL-97 [32]. All the non-hydrogen atoms except furyl ring in **2** were refined anisotropically and the hydrogen atoms were refined isotropically. In **2**, the furyl (C10–C13 and O1) ring was disordered over two positions. Details of the crystal data and structure refinement parameters for **2** and **3** are summarized in Table 5. Selected bond lengths and angles are summarized in Table 6.

4.2. Preparation of N-furfuryl-N-(2-phenylethyl)amine

2-Phenylethylamine (0.6 mL, 4.6 mmol) and furfuraldehyde (0.4 mL, 5.1 mmol) were dissolved in methanol (10 mL) and the solution was stirred for 2 h at room temperature. The solvent was removed by evaporation. The resulting yellow oil was dissolved in methanol–dichloromethane solvent mixture (1:1, 20 mL) and sodium borohydride (0.5 g, 13.8 mmol) was added slowly at 5 °C. The mixture was stirred at room temperature for 24 h. After evaporation of the solvent, the resulting viscous liquid was washed with water and dichloromethane was added in order to extract the product. Evaporation of the organic layer gave *N*-furfuryl-*N*-(2-phenylethyl) amine as a yellow oil.

^{1}H NMR (400 MHz, $CDCl_3$): δ 2.17 (b, 1H, NH), 2.72 (t, J = 6.6 Hz, 2H, N–CH_2–$C\underline{H}_2$), 2.79 (t, J = 6.4 Hz, 2H, N–$C\underline{H}_2$–CH_2), 3.68 (s, 2H, N–CH_2 (furfuryl)), 6.07–7.26 (aryl–H, m, 5H (phenyl)). ^{13}C NMR (100 MHz, $CDCl_3$): δ 36.2 (N–CH_2–$\underline{C}H_2$), 46.0 (N–$\underline{C}H_2$–CH_2), 50.3 (N–CH_2 (furfuryl)), 107.0, 110.2, 110.4, 126.3, 128.5, 128.8, 141.8, 142.0, 142.6, 153.8 (aryl carbon).

4.3. [Zn(fpedtc)$_2$] (**1**)

N-Furfuryl-*N*-(2-phenylethyl)amine (0.87 g, 4 mmol) and carbon disulfide (0.3 mL, 4 mmol) were dissolved in ethanol (20 mL), and stirred for 30 min. $ZnSO_4 \cdot 7H_2O$ (0.58 g, 2 mmol) was dissolved in 10 mL of water and added to the solution with constant stirring. A white powder precipitated that was filtered and dried.

Yield: 80%. m.p. 140 °C. IR (KBr, cm^{-1}): 1014 (ν_{C-S}), 1487 (ν_{C-N}), 2926 ($\nu_{C-H(aliph.)}$), 3061 ($\nu_{C-H(arom.)}$). ^{1}H NMR (500 MHz, $CDCl_3$): δ 3.02 (t, J = 8.0 Hz, 4H, N–CH_2–$C\underline{H}_2$), 4.04 (t, J = 8.0 Hz, 4H, N–$C\underline{H}_2$–CH_2), 4.95 (s, 4H, N–CH_2 (furfuryl)), 6.38 (dd, J = 2.0, 3.5 Hz, 2H, H-4 (furyl)), 6.44 (d, J = 3.0 Hz, 2H, H-3 (furyl)), 7.22–7.33 (m, 10H (phenyl)), 7.42 (d, J = 2.0 Hz, 2H, H-5 (furyl)). ^{13}C NMR (125 MHz, $CDCl_3$): δ 32.9 (N–CH_2–$\underline{C}H_2$), 51.2 (N–$\underline{C}H_2$–CH_2), 55.8 (N–CH_2 (furfuryl)), 110.5, 110.8, 126.8, 128.8, 128.9, 137.9, 142.9, 148.2 (aryl carbon), 205.2 (CS_2). Anal. Calc. for $C_{28}H_{28}S_4N_2O_2Zn$ (%): C, 54.40; H, 4.56; N, 4.53. Found (%): C, 54.28; H, 4.48; N, 4.49.

4.4. [Zn(fpedtc)$_2$(py)] (**2**)

The pyridine adduct was prepared by dissolving the complex **1** in warm pyridine. The yellow solution obtained was filtered and kept for evaporation. After few days both powder and single crystals separated out.

Yield: 60%. m.p. 110 °C. IR (KBr, cm^{-1}): 1017 (ν_{C-S}), 1478 (ν_{C-N}), 1604 (py), 2936 ($\nu_{C-H(aliph.)}$), 3074 ($\nu_{C-H(arom.)}$). ^{1}H NMR (500 MHz, $CDCl_3$): δ 3.02 (t, J = 10.0 Hz, 4H, N–CH_2–$C\underline{H}_2$), 4.07 (t, J = 10.0 Hz, 4H, N–$C\underline{H}_2$–CH_2), 5.06 (s, 4H, N–CH_2 (furfuryl)), 6.36 (dd, J = 2.5, 4.0 Hz, 2H, H-3 (furyl)), 6.43 (d, J = 3.5 Hz, 2H, H-4 (furyl)), 7.40 (d, J = 3.5 Hz, 2H, H-5 (furyl)), 7.18–7.31 (m, 10H (phenyl)), 7.47 (t, J = 2.8 Hz, 2H, H-3 (py)), 7.88 (t, J = 6.1 Hz, 1H, H-4 (py)), 9.01 (d, J = 6 Hz, 2H, H-2 (py)). ^{13}C NMR (125 MHz, $CDCl_3$): δ 32.8 (N–CH_2–$\underline{C}H_2$), 51.2 (N–$\underline{C}H_2$–CH_2), 55.8 (N–CH_2 (furfuryl)), 110.0, 110.6,

Table 3
Antifungal activity (diameter of inhibition zone (cm)) of complexes **1**–**4** against four different fungal pathogens.

Selected fungi	Chloramphenicol (100 μg)	Complex				Disc content (μg/disc)
		1	**2**	**3**	**4**	
Microsporum gypseum	1.6	1.5	0.5	–	1.0	100
		1.9	0.8	1.2	1.2	400
Trichophyton rubrum	1.9	0.8	0.5	0.7	0.6	100
		1.2	1.2	0.8	1.2	400
Epidermophyton floccosum	2.0	0.4	0.5	–	0.4	100
		0.8	0.9	0.6	0.6	400
Trichophyton mentagrophyte	2.2	0.7	0.8	0.4	1.5	100
		1.3	1.3	1.3	1.6	400

Table 4
Anticancer effect of complexes **1**–**4** on HeLa cell line.

Concentration of complex (μg/mL)	Cell viability (%) of the complexes			
	1	2	3	4
10	13.3	91.6	95.8	91.6
20	13.3	85.4	93.7	89.5
30	13.3	81.2	85.4	85.4
40	6.7	75.0	79.1	75.0
50	6.7	66.6	66.6	70.8

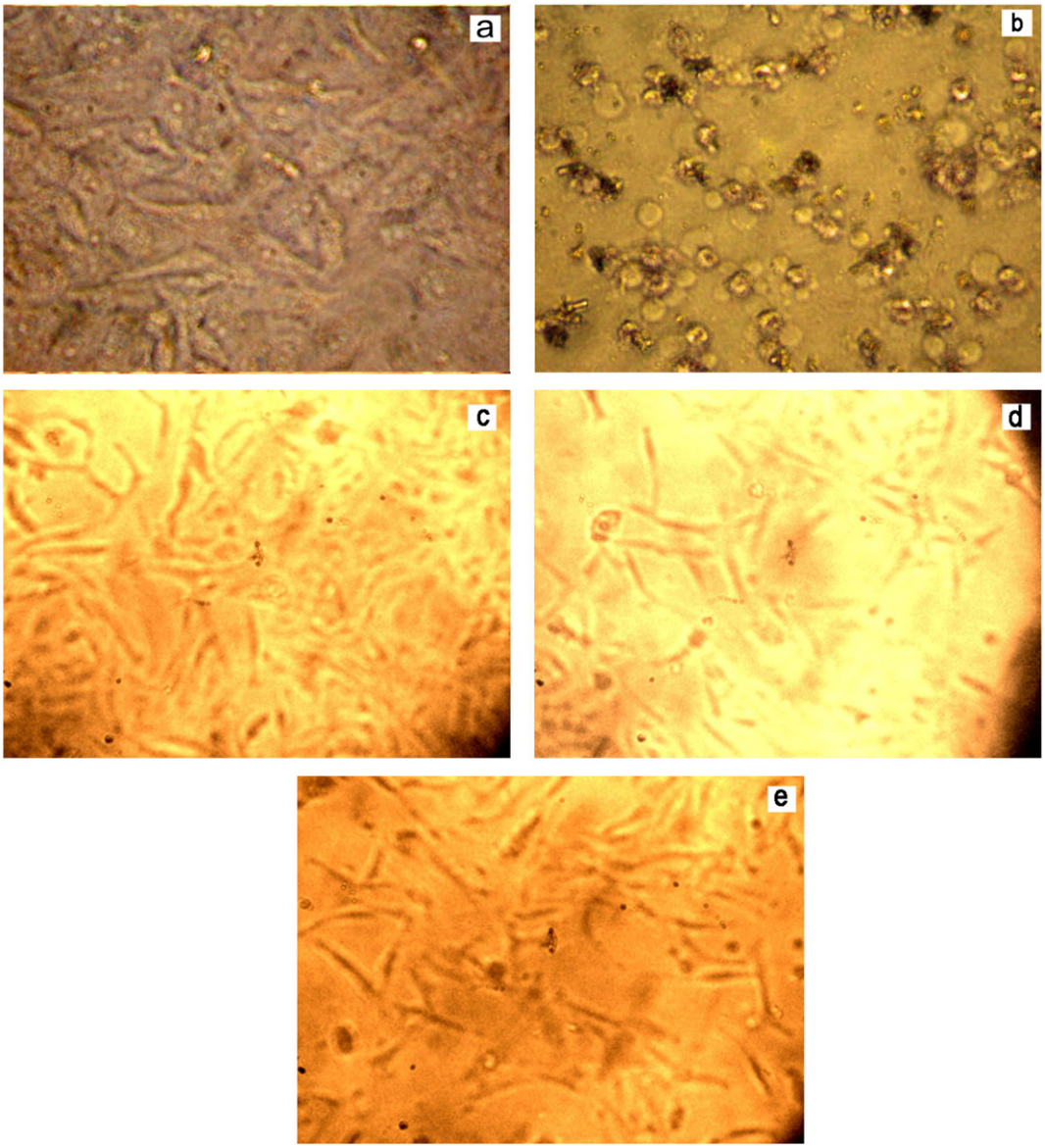

Fig. 4. (a) Control cancer cells. Apoptotic morphological changes were observed in the cells treated with 50 μg/mL of complexes (b) **1** (c) **2** (d) **3** and (e) **4**.

124.7, 126.5, 128.5, 128.8, 138.4, 142.5, 149.0, 149.4 (aryl carbon), 206.5 (CS_2). Anal. Calc. for $C_{33}H_{33}N_3S_4O_2Zn$ (%): C, 56.84; H, 4.76; N, 6.02. Found (%): C, 56.69; H, 4.68; N, 5.96.

4.5. *[Zn(fpedtc)$_2$(1,10-phen)] (**3**)*

Adduct was prepared by adding a hot solution of 1,10-phenanthroline (2 mmol) in ethanol to a hot solution of complex **1** (1 mmol) in chloroform. The resulting solution was cooled and then added with petroleum-ether (boiling range: 40–60 °C). Yellow precipitate of the adduct was separated out. Suitable single crystals for X-ray structure analysis were obtained by repeated crystallization from dichloromethane–benzene solvent mixture.

Yield: 80%. m.p. 162 °C. IR (KBr, cm^{-1}): 1014 (ν_{C-S}), 1462 (ν_{C-N}), 1507, 1584 (1,10-phen), 2928 ($\nu_{C-H(aliph.)}$), 3063 ($\nu_{C-H(arom.)}$). ^{1}H NMR (500 MHz, $CDCl_3$): δ 3.03 (t, J = 8.0 Hz, 4H, N–CH_2–CH_2), 4.10 (t, J = 8.3 Hz, 4H, N–CH_2–CH_2), 5.12 (s, 4H, N–CH_2 (furfuryl)), 6.33 (dd, J = 2.0, 3.5 Hz, 2H, H-4 (furyl)), 6.40 (d, J = 3.0 Hz, 2H, H-3 (furyl)), 7.20–7.29 (m, 10H (phenyl)), 7.36 (d, J = 2.0 Hz, 2H, H-5 (furfuryl)), 7.87 (b, 4H, H-3 (1,10-phen)), 7.94 (s, 2H, H-5 (1,10-phen)), 8.45 (d, J = 1.5 Hz, 2H, H-4 (1,10-phen)), 9.75 (d, J = 4 Hz, 2H, H-2 (1,10-phen)). ^{13}C NMR (125 MHz, $CDCl_3$): δ 32.8 (N–CH_2–CH_2), 51.3 (N–CH_2–CH_2), 55.7 (N–CH_2 (furfuryl)), 109.4, 110.5, 124.7, 126.2, 126.6, 128.5, 128.7, 128.9, 137.8, 138.9, 141.3, 142.2, 149.1, 150.0 (aryl carbon), 207.1 (CS_2). Anal. Calc. for $C_{40}H_{36}N_4S_4O_2Zn$ (%): C, 60.17; H, 4.54; N, 7.01. Found (%): C, 60.11; H, 4.47; N, 6.96.

4.6. *[Zn(fpedtc)$_2$(2,2′-bipy)] (**4**)*

A method similar to that described for the synthesis of **3** was adopted, however, 2,2′-bipyridine (2 mmol) was used instead of 1,10-phenanthroline. Yellow precipitate of adduct was separated out.

Yield: 70%. m.p. 158 °C. IR (KBr, cm^{-1}): 1017 (ν_{C-S}), 1468 (ν_{C-N}), 1567, 1600 (2,2′-bipy), 2925 ($\nu_{C-H(aliph.)}$), 3063 ($\nu_{C-H(arom.)}$). ^{1}H NMR (400 MHz, $CDCl_3$): δ 3.00 (t, J = 8.0 Hz, 4H, N–CH_2–CH_2), 4.05 (t, J = 8.0 Hz, 4H, N–CH_2–CH_2), 5.01 (s, 4H, N–CH_2 (furfuryl)), 6.35 (b, 2H, H-4 (furyl)), 6.41 (d, J = 2.8 Hz, 2H, H-3 (furyl)), 7.19–7.31 (m, 10H

Table 5
Crystal data, data collection and refinement parameters for **2** and **3**.

	2	**3**
Empirical formula	$C_{33}H_{33}N_3O_2S_4Zn$	$C_{40}H_{36}N_4O_2S_4Zn$
FW	697.23	798.34
Temperature	293(2) K	293(2) K
Wavelength	0.71073 Å	0.71073 Å
Crystal system	Monoclinic	Monoclinic
Space group	*C*2	*P*21/*n*
Unit cell dimension		
a (Å)	32.6725(9)	15.5871(7)
b (Å)	8.4874(2)	14.2405(7)
c (Å)	6.0549(2)	17.0145(8)
β (°)	91.752(2)	97.1190(10)
Absorption coefficient	1.014 mm^{-1}	0.919 mm^{-1}
F(000)	724	1656
Crystal size	0.25 × 0.20 × 0.15 mm	0.30 × 0.25 × 0.20 mm
θ Range (°)	1.25–27.50	1.87–29.52
Limiting indices	$-42 \le h \le 42$, $-8 \le k \le 11$, $-7 \le l \le 7$	$-21 \le h \le 21$, $-19 \le k \le 19$, $-23 \le l \le 23$
Reflections collected/unique	9236/3253 [*R*(int) = 0.0200]	47,543/10,433 [*R*(int) = 0.0393]
Absorption correction	Semi-empirical from equivalents	Semi-empirical from equivalents
Max. and min. transmission	0.8627 and 0.7856	0.8375 and 0.7700
Refinement method	Full-matrix least-squares on F^2	Full-matrix least-squares on F^2
Data/restraints/parameters	3253/39/210	10,433/0/461
Goodness-of-fit on F^2	1.136	1.041
Final *R* indices [$I > 2\sigma(I)$]	$R_1 = 0.0275$, $wR_2 = 0.0771$	$R_1 = 0.0397$, $wR_2 = 0.0985$
R indices (all data)	$R_1 = 0.0317$, $wR_2 = 0.0893$	$R_1 = 0.0790$, $wR_2 = 0.1249$
Largest diff. peak and hole	0.257 and −0.398 e $Å^{-3}$	0.424 and −0.301 e $Å^{-3}$

(phenyl)), 7.39 (b, 2H, H-5 (furyl)), 7.44 (t, $J = 1.8$ Hz, 2H, H-4 (2,2′-bipy)), 7.91 (t, $J = 7.2$ Hz, 2H, H-5 (2,2′-bipy)), 8.29 (d, $J = 5.6$ Hz, 2H, H-6 (2,2′-bipy)), 9.03 (b, 2H, H-3 (2,2′-bipy)). ^{13}C NMR (100 MHz, $CDCl_3$): *δ* 32.9 (N–CH_2–$\underline{C}H_2$), 51.3 (N–$\underline{C}H_2$–CH_2), 55.8 (N–CH_2 (furfuryl)), 110.0, 110.7, 120.9, 124.6, 126.6, 128.6, 128.9, 137.9, 138.4, 142.6, 149.0, 149.3 (aryl carbon), 206.5 (CS_2). Anal. Calc. for $C_{38}H_{36}N_4S_4O_2Zn$ (%): C, 58.9; H, 4.68; N, 7.23. Found (%): C, 58.72; H, 4.63; N, 7.19.

4.7. Antimicrobial screening

The antimicrobial activity of the synthesized complexes was tested against some Gram-positive and Gram-negative bacteria and fungi. The activity of the compounds was compared with standard reference drug. Minimum inhibitory concentration of the complexes was tested in Sabourauds dextrose broth (SDB) for fungi and in Nutrient broth (NB) for bacteria by the two-fold serial dilution method [33]. Seeded broth (broth containing microbial spores) was prepared in NB from 24 h old bacterial cultures on nutrient agar (Hi-media, India) at 37 ± 1 °C while fungal spores from 24 h to 7 days old Sabourauds agar slant cultures were suspended in SDB. The bacterial suspension was adjusted with sterile saline to a concentration of 1×10^4–10^5 CFU. The tested compounds and reference drugs were prepared by two-fold serial dilution to obtain the required concentrations of 200, 100, 50, 25, 12.5, 6.25 and 3.12 μg/mL. The tubes were incubated in BOD incubators at 37 ± 1 °C for bacteria and 28 ± 1 °C for fungi. The minimum inhibitory concentrations (MICs) were recorded by visual observations after 24 h (for bacteria) and 72–96 h (for fungi) of incubation. Chloramphenicol was used as standard drug.

Table 6
Selected bond lengths (Å) and bond angles (°) of **2** and **3**.

2		**3**	
Bond length			
Zn1–N2	2.025(4)	Zn1–S1	2.4936(7)
Zn1–S1	2.3600(7)	Zn1–S2	2.5291(6)
Zn1–S2	2.5621(6)	Zn1–S3	2.4507(7)
C14–S1	1.721(2)	Zn1–S4	2.6267(7)
C14–S2	1.702(3)	Zn1–N3	2.1676(18)
C14–N1	1.339(3)	Zn1–N4	2.2156(8)
		C1–S1	1.711(2)
		C1–S2	1.710(2)
		C1–N1	1.347(3)
		C15–S3	1.716(2)
		C15–S4	1.711(2)
		C15–N2	1.339(3)
Bond angle			
S2–Zn1–$S2^i$	167.02(4)	S1–Zn1–S2	71.60(2)
S1–Zn1–$S1^i$	133.07(4)	S1–Zn1–S4	100.99(2)
S1–Zn1–S2	73.07(2)	S2–Zn1–S4	170.54(2)
		S2–C1–S1	118.38(13)
		S3–Zn1–S4	70.77(2)
		S4–C15–S3	118.39(13)
		N6–Zn1–N5	75.18(7)

4.8. Antibacterial assay (disc diffusion method)

The disc diffusion assay was used to determine antibacterial activity of the complexes using *Gram-positive* and *Gram-negative* strains of bacteria *viz*., *E. coli*, *S. typhi*, *V. cholerae* and *S. aureus*. Base plates were prepared by pouring 10 mL of autoclaved Muller-Hinton agar into sterile petridishes (9 cm) and allowed them to settle. Sterile blank discs (6 mm) were impregnated with 15 μL of known concentration of stock solution of tested complexes as to obtain discs containing 100 and 400 μg of each complexes. Impregnated discs were air dried and cautiously placed on the surface of Mueller-Hinton agar plates freshly inoculated with microorganisms. After 10 min at room temperature the plated culture incubated for 24 h at 37 °C. Experiments were conducted in quadruplicate (four discs with identical concentration of the same compound) and commercial antibiotic Chloramphenicol (100 μg) impregnated discs used as positive controls. Susceptibility diameter zone was reported as the average value of replicate measurements.

4.9. Antifungal screening (disc diffusion method)

A disc application technique was employed *in vitro* to evaluate the antifungal activity of synthesized complexes. Antifungal

activity of the complexes were tested against *M. gypseum*, *T. rubrum*, *E. floccosum* and *T. mentagrophyte*. Mature conidia of fungal isolates were harvested from potato dextrose agar (PDA) plates and suspended in ringer solution and spore suspensions standardized with a haemocytometer (10^4 conidia mL^{-1}). Conidial suspension (1 mL) representing each fungal isolate was then spread on a 9 cm petridishes containing PDA (20 mL) with the excess of conidial suspension decanted and allow to dry. The compounds were dissolved in dimethyl sulfoxide (DMSO). Sterile 6 mm diameter test discs were impregnated with 15 μL of the solution of each test compound to certain 100 and 400 μg/disc in triplicates. Chloramphenicol was used as a reference drug, for fungal inhibition. While DMSO was used as a negative control. Plates were incubate at room temperature (22–25 °C) for 3 days. The radius of the inhibition zone of fungal growth was measured after 3 days. Diameter zone was reported.

4.10. Anticancer activity

4.10.1. Cell lines and culture conditions

HeLa cell lines were obtained from King Institute, Guindy, Chennai. The growth medium was supplemented with antibiotics penicillin, streptomycin and 10% complemented fetal bovine serum. The growth of all the cell cultures was accomplished in 25 mL Falcon bottles at 37 °C under continuous flux of a 5% CO_2 and moisture enriched atmosphere.

4.10.2. MTT assay

Tetrazolium salt reduction test was undertaken according to the method described by Alley et al. [34]. 5×10^3 cells mL^{-1} for HeLa cells were seeded in 96-well microplates in the appropriate growth medium (100 μL) and then incubated at 37 °C in a 10% carbon dioxide controlled atmosphere. After 24 h, the medium was removed and replaced with a fresh medium containing the complex, to be studied previously dissolved in DMSO, at increasing concentrations (10, 20, 30, 40 and 50 μg mL^{-1}). Triplicate cultures were established for each treatment. After 24 h, each well was treated with 10 μL of a 5 mg mL^{-1} MTT (3-(4,5-dimethylthiazol-2-yl)-2,5-diphenyltetrazolium bromide, Sigma Chemical Co.) saline solution and after 5 h of incubation, in 0.1 M HCl solution was added. After 4 h incubation, 0.04 M HCl/isopropanol were added. Viable cells were determined by the absorbance at 570 nm. The absorbance at 570 nm was measured with a UV-spectrophotometer using wells without sample containing cells as blanks. The effect of the samples on the proliferation of HeLa was expressed as the % cell viability, using the following formula:

$$\%\ \text{Cell viability} = \text{A570 of treated cells}/\text{A570 of control cells} \times 100\%.$$

Acknowledgments

We are thankful to SAIF, Indian Institute of Technology-Madras, Chennai, India for the single crystal X-ray structural analysis.

Appendix A. Supplementary data

The crystallographic data for the structural analysis of complexes **2** and **3** have been deposited with the Cambridge Crystallographic Data Centre, CCDC No. for **2** is 886788 and for **3** is 886787. Copy of this information may be obtained free of charge from the Director, CCDC, 12 Union Road, Cambridge CB2 1EZ, UK (Tel.: +44 (0) 1223 762911; E-mail: kamila@ccdc.cam.ac.uk).

References

[1] S. Fujii, T. Yoshimura, A new trend in iron-dithiocarbamate complexes: as an endogenous NO trapping agent, Coord. Chem. Rev. 198 (2000) 89–99.
[2] M.J. Cox, E.R.T. Tiekink, The diverse coordination patterns in the structures of zinc, cadmium and mercury bis(1,1-dithiolates), Rev. Inorg. Chem. 17 (1997) 1–23.
[3] L. Marcheselli, C. Preti, M. Tagliazucchi, V. Cherchi, L. Sindellari, A. Furlani, A. Papaioannou, V. Scarcia, Synthesis, characterization and evaluation of biological activity of palladium(II) and platinum(II) complexes with dithiocarbamic acids and their derivatives as ligands, Eur. J. Med. Chem. 28 (1993) 347–352.
[4] L. Batemann, The Chemistry and Physics of Rubber-like Substance, McClaren, London, 1963.
[5] R. Becker, A. Knorr, An evaluation of antioxidants for vegetable oils at elevated temperatures, Lubr. Sci. 8 (1996) 95–117.
[6] N. Srinivasan, S. Thirumaran, Effect of pyridine as a ligand in precursor on morphology of CdS nanoparticles, Superlattices Microstruct. 51 (2012) 912–920.
[7] P. Yan, Y. Xie, Y. Qian, X. Liu, A cluster growth route to quantum-confined CdS nanowires, Chem. Commun. (1999) 1293–1294.
[8] D. Coucouvanis, The chemistry of the dithioacid and 1,1-dithiolate complexes, 1968-1977, in: S.J. Lippard (Ed.), Progress in Inorganic Chemistry, vol. 26, John Wiley and Sons, Inc., 1979, pp. 301–469.
[9] G. Hogarth, Transition metal dithiocarbamates: 1978–2003, in: K.D. Karlin (Ed.), Progress in Inorganic Chemistry, vol. 53, John Wiley and Sons, Inc., 2005, pp. 71–561.
[10] M.J. Burkitt, H.S. Bishop, L. Milne, S.Y. Tsang, G.J. Provan, C.S.I. Nobel, S. Orrenius, A.F.G. Slater, Dithiocarbamate toxicity toward thymocytes involves their copper-catalyzed conversion to thiuram disulfides, which oxidize glutathione in a redox cycle without the release of reactive oxygen species, Arch. Biochem. Biophys. 353 (1998) 73–84.
[11] A.K. Malik, W. Faubel, Methods of analysis of dithiocarbamate pesticides: a review, Pestic. Sci. 55 (1999) 965–970.
[12] E. Humeres, N.A. Debacher, M.M. de S. Sierra, Mechanisms of acid decomposition of dithiocarbamates. 2. Efficiency of the intramolecular general acid catalysis, J. Org. Chem. 64 (1999) 1807–1813.
[13] T. Kamenosono, H. Shimada, T. Funakoshi, S. Kojima, Involvement of active transport systems in the mobilization of cadmium by dithiocarbamates *in vivo*, Toxicology 170 (2002) 103–110.
[14] G.M. Noordhuis, J.H. Jasper, E.F. Roossink, P.D. Graeff, H. Geertruida, Prognostic cell biological markers in cervical cancer patients primarily treated with (chemo) radiation: a systematic review, Int. J. Radiat. Oncol. 79 (2011) 325–334.
[15] L.H. Ellenson, T.C. Wu, Focus on endometrial and cervical cancer, Cancer Cell 5 (2004) 533–538.
[16] B. Lippert, Impact of cisplatin on the recent development of Pt coordination chemistry: a case study, Coord. Chem. Rev. 182 (1999) 263–295.
[17] M. Galanski, M.A. Jakupec, B.K. Keppler, Update of the preclinical situation of anticancer platinum complexes: novel design strategies and innovative analytical approaches, Curr. Med. Chem. 12 (2005) 2075–2094.
[18] S. Hidaka, M. Tsuruoka, T. Funakoshi, H. Shimada, M. Kiyozumi, S. Kojima, Protective effects of dithiocarbamates against renal toxicity of *cis*-diamminedichloroplatinum in rats, Ren. Fail. 16 (1994) 337–349.
[19] D.L. Bodenner, P.C. Dedon, P.C. Keng, R.F. Borch, Effect of diethyldithiocarbamate on *cis*-diamminedichloroplatinum(II)-induced cytotoxicity, DNA cross-linking, and γ-glutamyl transpeptidase inhibition, Cancer Res. 46 (1986) 2745–2750.
[20] E.M. Walker Jr., R.F. Schaefer, K.J. Henle, B.J. Schmidt, G.R. Gale, D.J. Cannon, M.M. Jones, A.J. Moss Jr., Combination and individual antitumor effects of hyperthermia, cisplatin, and selected dithiocarbamates, Ann. Clin. Lab. Sci. 19 (1989) 242–254.
[21] E.R.T. Tiekink, Molecular architecture and supramolecular association in the zinc-triad 1,1-dithiolates. Steric control as a design element in crystal engineering? CrystEngComm 5 (2003) 101–113.
[22] R. Kant, V.K. Gupta, K. Kapoor, P. Valarmathi, S. Thirumaran, Bis(μ-*N*-benzyl-*N*-furfuryldithiocarbamato)-1:2κ^3S, S′:S′;2:1κ^3S, S′:S′-bis[(*N*-benzyl-*N*-furfuryldithiocarbamato-κ^2S, S′)cadmium], Acta Crystallogr. E 68 (2012) m12–m13.
[23] F. Bonati, R. Ugo, Organotin(IV) N, N-disubstituted dithiocarbamates, J. Organomet. Chem. 10 (1967) 257–268.
[24] D.C. Bradley, M.H. Gitlitz, Preparation and properties of *NN*-dialkyldithiocarbamates of early transition elements, J. Chem. Soc. A (1969) 1152–1156.
[25] S. Thirumaran, K. Ramalingam, G. Bocelli, A. Cantoni, Electron density distribution studies on ZnS_4N_2 chromophore in solution and solid phases: XPS and cyclic voltammetric studies on 1,10-phenanthroline and 2,2′-bipyridine adducts of bis(piperidinecarbodithioato-S, S′)zinc(II). Single crystal X-ray structure of (2,2′-bipyridine)bis(piperidinecarbodithioato-S, S′)zinc(II), Polyhedron 18 (1999) 925–930.
[26] B. Martin, W.R. McWhinnie, G.M. Waind, 2:2′-Dipyridyl complexes of cobalt, rhodium and iridium-II: low-valent rhodium complexes, J. Inorg. Nucl. Chem. 23 (1961) 207–223.
[27] A.W. Addison, T. Nageswara Rao, J. Reedijk, J. van Rijn, G.C. Verschoor, Synthesis, structure, and spectroscopic properties of copper(II) compounds containing nitrogen-sulphur donor ligands; the crystal and molecular structure of

aqua[1,7-bis(*N*-methylbenzimidazol-2′-yl)-2,6-dithiaheptane]copper(II) perchlorate, J. Chem. Soc. Dalton Trans. (1984) 1349–1356.
[28] F. Shaheen, C. Gieck, A. Badshah, M.K. Khosa, Bis(μ-piperidine-1-dithiocarboxylato-κ^2S: S′)[bis(piperidine-1-dithiocarboxylato-κ^2S, S′)zinc(II)], Acta Crystallogr. E 62 (2006) m1186–m1187.
[29] P.B. Sreeja, M.R.P. Krup, A. Kishore, C. Jasmin, Spectral characterization, X-ray structure and biological investigations of copper(II) ternary complexes of 2-hydroxyacetophenone 4-hydroxybenzoic acid hydrazone and heterocyclic bases, Polyhedron 23 (2004) 575–581.
[30] K.C. Mollay, in: F.E. Hartley (Ed.), The Chemistry of Metal Carbon Bond, Wiley, New York, 1989.
[31] A. Altomare, G. Cascarano, C. Giacovazzo, A. Guagliardi, M.C. Burla, G. polidori, M. Camalli, J. Appl. Crystallogr. 27 (1994) 435–436.
[32] G.M. Sheldrick, SHELXL-97, University of Gottingen, Germany, 1997.
[33] National Committee for Clinical Laboratory Standards Methods for Dilution Antimicrobial Susceptibility Tests for Bacteria that Grow Aerobically, fifth ed., National Committee for Clinical Laboratory Standards, Villanova, PA, 2000, Approved Standard. NCCLS Document M7–A5.
[34] M.C. Alley, D.A. Scudiero, A. Monks, M.L. Hursey, M.J. Czerwinski, D.L. Fine, B.J. Abbott, J.G. Mayo, R.H. Shoemaker, M.R. Boyd, Feasibility of drug screening with panels of human tumor cell lines using a microculture tetrazolium assay, Cancer Res. 48 (1988) 589–601.